

# To Boldly Go Where No Robots Have Gone Before – Part 1: EELS Robot to Spearhead a New One-Shot Exploration Paradigm with In-situ Adaptation

Masahiro Ono, Rohan Thakker, Nikola Georgiev, Peter Gavrillov, Avak Archanian, Tomas Drevinskas, Guglielmo Daddi, Michael Paton, Marlin Strub, Hovhannes Melikyan, Torkom Pailevanian, Rob Royce, R. Michael Swan, Christopher Lopez, Eric Ambrose, Bryson Jones, Christiahn Roman, Luis Phillippe Tosi, Richard Rieber, Matthew Gildner, Benjamin Hockman, Daniel Loret de Mola Lemus, Daniel Paster Moreno, Tristan D. Hasseler, Tiago Stegun Vaquero, Marcel Veismann, Yashwanth Kumar Nakka, Eloise Marteau, Sarah Yearicks, Sina Aghli, Benjamin Nuernberger, Martin Peticco, Morgan Cable, Pedro Proenca, Michael Malaska, Gregory Agnes, Mirza Samnani, Joseph Bowkett, Baylor de los Reyes, Marco Tempest, Lori Shiraishi, Ashkan Jasour, Tony Tran, Michel Ingham, Jeremy Nash, Linda Spilker, Dan Balentine, Ansel Barchowsky, Fredrik Bevreng, Kyle Botteon, Kyle Brown, Matthew Caballero, Kalind Carpenter, Mark Chodas, Adriana Daca, Sierra Dacey, Hendrik Dreger, Jason Feldman, Alex Gardner, Austen Goddu, Jenna Holland, Abhinandan Jain, Jay Jasper, Curtis Jin, Maisha Khanum, Richard Kornfeld, Carl Leake, Gary Mark, Benjamin Morrell, Jack Naish, William Reid, Jacob Rodriguez, William Talbot, Jessica Weber, Malcom Wright, Harshad Zade, Jenny Zhang, Rachel Etheredge, and Matthew Robinson

*Jet Propulsion Laboratory, California Institute of Technology, Pasadena, CA, 91109, USA*

**Abstract:** Historically, robotic space exploration has been conducted in a sequence of incrementally more sophisticated missions, starting with flyby and orbiting, followed by simple landing and roving missions, and eventually leading to more complex robotic missions involving long-range driving, drilling, or sample return. The benefit of this approach is that capabilities can be specifically designed for narrowly defined environmental conditions. For example, the development and V&V of the complex robotic functions of NASA’s Mars rover *Perseverance*, such as autonomous driving and the sampling and caching system, were heavily informed by the environmental knowledge gained from previous Mars missions. However, now that NASA is destined to explore a multitude of more challenging worlds, we will likely not enjoy the luxury of sending a series of spacecraft to the same destination due to budgetary constraints, a scarcity of flight opportunities, and the extensive cruise time to the Outer Solar System and beyond. We argue that a new robotic exploration paradigm will be needed, which replaces an incremental exploration campaign with a single-shot mission where a robot or a team of robots adapts its behavior *after* arrival and increasingly elevates the level of behavioral complexity as it learns about the new environment. A key enabler of such adaptive one-shot exploration is highly versatile robotic hardware combined with onboard intelligence. We have developed a snake-like versatile and intelligent robot, namely the *Exobiology Extant Life Surveyor* or *EELS*, which would enable access to the subsurface oceans of icy moons by descending into an erupting vent, such as those on Enceladus. By combining its high-DOF mechanical system (Gildner, et al. 2024), active skin propulsion system (Marteau, et al. 2024), and the new adaptive autonomy software framework called *NEO Autonomy* (Thakker, Paton, et al. 2023), we demonstrated through numerous lab and field tests that EELS can locomote in a wide range of environmental conditions, including sand-covered surface, undulating ice, high-slope snow, and vertical glacial shafts, by switching between significantly different mobility gaits. It is particularly notable that EELS achieved ~1.5 m fully autonomous vertical descents in the natural ice moulins of Athabasca Glacier in Canada. This paper first highlights the limitations of the current incremental exploration paradigm and builds an argument for the adaptive, one-shot exploration paradigm by drawing insights from a number of flight and research projects. We will then provide a broad overview of the vision, technologies, scientific impacts, capabilities, and field test results of EELS, while the three companion papers (Gildner, et al. 2024), (Marteau, et al. 2024), and (Thakker, Paton, et al. 2023) provide the detailed description of the hardware, active skin propulsion, and autonomy systems of EELS, respectively.

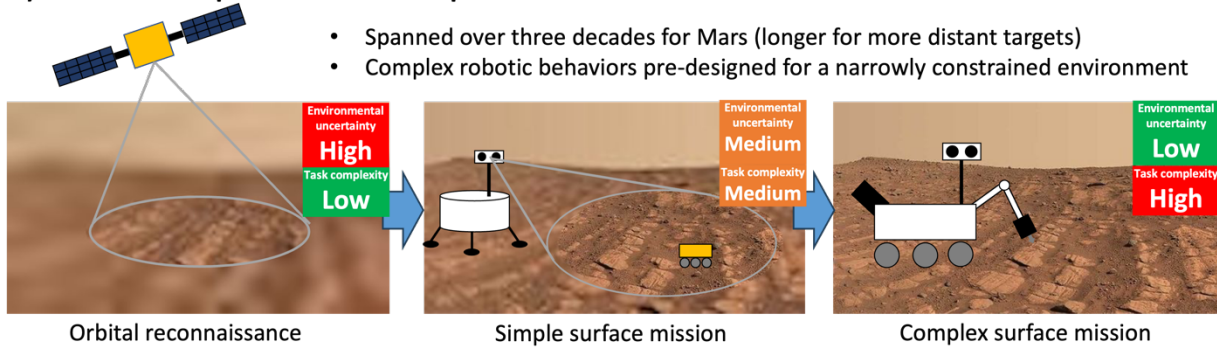
## I. Introduction – A brief history of paradigm changes in robotic space exploration

Robotic space exploration has been at the forefront of scientific discovery for more than six decades, driving humanity to uncover the mysteries of the cosmos. Its essence has been, and will be, unchanged: *turning unknowns into knowns*. What *has* changed, though, is our approach to turning unknowns into knowns. To put it another way, the reason we have been able to push the frontier of exploration over six decades is that we reinvented the way to explore space multiple times.

Take, for example, NASA’s pre-Apollo Lunar missions in the late 1950s to 1960s. Their approach to turning unknowns at that time was rapidly iterating trial and error cycles. NASA launched 20 spacecraft during the decade, or at a six-month interval on average. The intervals were often merely a month or two (e.g., Pioneer 1-4; Ranger 1-3, Surveyor 3-4). Moreover, sometimes it was not just a relaunch of identical spacecraft, but enhancements were rapidly implemented within an interval of only a few months (e.g., Ranger 2 and 3). Flight projects at that time operated very differently from today. All the first ten missions (Pioneer 1-4; Ranger 1-6) failed, with an overall success rate of 40%. NASA and the Jet Propulsion Laboratory, which built and operated the missions, quickly learned from failures and eventually landed five Surveyor landers on the Moon successfully, which played a critical role as the precursor to Apollo. This “try again, fail again, fail better”<sup>1</sup> paradigm was adequate for the Moon because of the short flight time (~3 days) and the frequent launch opportunities.

The same paradigm does not work for interplanetary missions. The relatively long cruise times (e.g., 6-7 months for Mars) and infrequent launch opportunities (e.g., once every 26 months for Mars) make rapid trial-and-error practically impossible. This may be the primary reason NASA (and other space agencies) switched to a more risk-averse paradigm after the conclusion of the pre-Apollo Lunar missions. For example, in the ongoing robotic Mars

### A) Incremental exploration with multiple missions



### B) One-shot exploration with *in-situ* adaptation

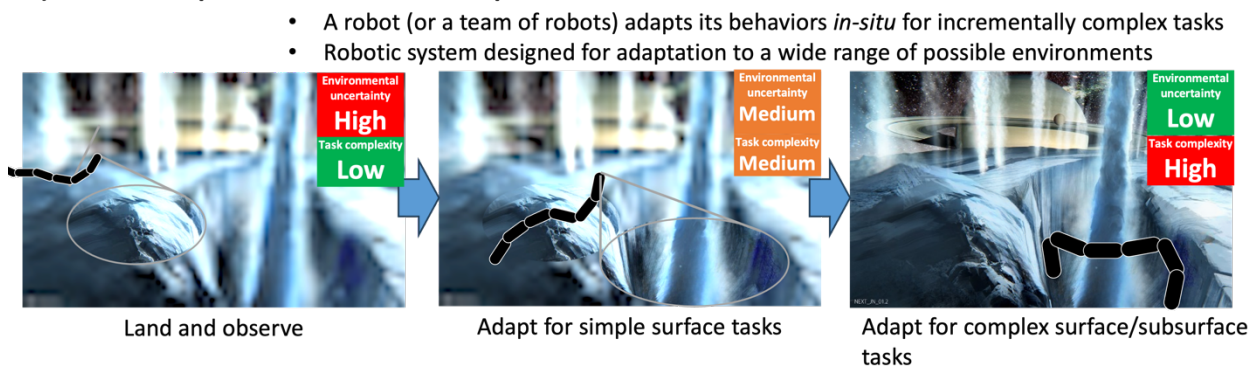


**Figure 1** The proposed paradigm change for enabling complex robotic missions beyond Mars. A) NASA has sent a series of missions that incrementally built up the complexity, but we will unlikely have the luxury of sending a series of spacecraft to each high-priority target beyond Mars. B) We argue that a one-shot mission can replace the conventional paradigm by sending a highly adaptive robot (or a team of robots) that changes the physical behavior as it learns about the unknown environment.

<sup>1</sup> Quote from Samuel Beckett

Exploration Program, which started in 1990, NASA/JPL-Caltech has launched 14 spacecraft over 30 years (~2-year intervals on average), of which 11 were successful<sup>2</sup>. As illustrated in Figure 1-A, this campaign is characterized by an incremental approach, which started with orbiters (e.g., Mars Global Surveyor, Mars Odyssey, Mars Reconnaissance Orbiter), followed by relatively simple surface missions (e.g., Mars Pathfinder, Mars Exploration Rovers), and evolved toward more complex missions (e.g., Mars Science Laboratory, Mars 2020, the planned Mars Sample Return campaign) that involve complicated robotic operations on the surface such as drilling and coring carefully selected rocks, autonomously driving over extensive distances, flying in the thin atmosphere, and transferring sample tubes between two robotic vehicles. Such an incremental approach has a clear benefit: as we sketch out in Section II with concrete examples from Mars 2020 and the planned Mars Sample Return missions, the complex robotic capabilities, which typically involve a greater level of risk to operate in an unknown environment, could be designed specifically for narrowly constrained environmental conditions, thanks to the data brought back by previous missions. This paradigm change from “try again, fail again” in the pre-Apollo Lunar missions to the cautiously incremental one was indeed one of the primary reasons for NASA/JPL’s tremendous success in Mars exploration.

However, such an incremental exploration approach is not applicable, or highly inefficient at best, for more challenging destinations beyond the surface of Mars. Firstly, the cruise time to the Outer Solar System, in which many of the high-priority targets in the latest Planetary Science and Astrobiology Decadal Survey are located, is very long (often ~10 years or more), while launch opportunities are highly limited primarily due to budgetary constraints. Secondly, the Outer Solar System alone includes a multitude of worlds to explore, such as centaurs, ice giants and their satellites, and KBOs. Unlike Mars exploration, we will not be able to enjoy the luxury of sending many spacecraft to a single target. A combined orbiter-lander (such as Enceladus Orbilander concept (MacKenzie, et al. 2021)) can provide detailed reconnaissance before the surface phase in a single mission, but the newly acquired environmental knowledge cannot be used for the design and V&V of the spacecraft before the launch. But perhaps more fundamentally, many scientifically interesting targets lay below the surface, where orbital reconnaissance is physically impossible (other than low-resolution mapping by ice/ground-penetrating radars). Examples include the lava tubes on the Moon and Mars, geysers on Enceladus and potentially on Europa (Sparks, et al. 2016) (Jia, et al. 2018), and the subsurface ocean of icy moons. We have two choices to move forward: to rely solely on low-risk missions (orbiters and basic landers), or to seek a new paradigm that enables single-shot missions with complex robotic tasks, such as autonomously roving over an extended range, collecting a diverse set of carefully selected samples, or even diving into the subsurface (Chodas, et al. 2023). This paper explores the latter option.

In the new one-shot exploration paradigm, a robotic explorer cannot be designed for narrowly constrained environmental conditions. Rather, it must be *built to adapt*. As we show with examples in Section III, adaptive robots are capable of resiliently performing complex robotic tasks under substantial environmental uncertainty. As illustrated in Figure 1-B, in the new paradigm, a robot, or a team of robots, would land in a poorly characterized environment and use its own sensors to observe it. As the environment is better understood, the robot(s) would adapt its behavior to perform simple robotic tasks, such as short-range/slow surface locomotion. As the environmental uncertainty is further reduced, it would adapt to perform more complex tasks, such as long-range traverse, sample collection, or subsurface mobility. We argue that the primary enablers are **i) versatile robotic hardware and ii) intelligent, risk-aware autonomy**. An adaptive robotic system, with single or multiple robots, will have to flexibly change the physical behaviors to interact with the environment (e.g., locomotion, sampling) after its arrival in an uncharacterized world. Furthermore, if the environment is not homogeneous or static (such as a region with an active plume), it will likely need to continuously adapt as new environmental conditions (e.g., different terrain types, changing topography) emerge. A non-versatile robot, which has a singular, pre-designed mode of interacting with the environment, will likely fail to cope with substantial environmental uncertainty. A versatile robot with multiple modes of mobility, sampling, and manipulation, combined with onboard autonomy for choosing the best mode based on the observed environmental conditions and the risks associated with it, will be a necessity.

The rest of the paper is structured in the following way. In Section II, we will investigate three concrete examples of complex robotic capabilities from the Mars 2020 rover and Mars Sample Return planning and reveal that the development and V&V process highly depended on the environmental knowledge brought by prior missions, hence necessitating the incremental exploration with a series of missions. Then, in Section III, we will propose a new one-shot exploration paradigm with an adaptive robotic system and argue with concrete examples that the key enabling technologies for the adaptive robotic system are hardware-level versatility and onboard intelligence. Section IV introduces EELS, our instantiation of the versatile and intelligent robotic system, which would enable access to subsurface oceans of icy moons and other challenging destinations. We present the hardware and software prototypes of EELS and summarize the outcome of lab and field tests, which demonstrate the adaptivity of EELS.

<sup>2</sup> It is also notable that the three failures occurred during NASA’s “faster, better, cheaper” era.

## II. Limitations of Incremental Exploration: Examples from Current Mars Missions

The Mars 2020 *Perseverance* rover and planned Mars Sample Return missions involve perhaps the most complex robotic systems ever sent to another planet. This section will take a deep dive into the development and V&V processes of several key robotic capabilities of these missions, and analyze how the environmental knowledge from past missions contributed. From there, we will discuss the limitations of the current incremental exploration paradigm.

### A. Enhanced AutoNav (ENav) of the Mars 2020 *Perseverance* Rover

The *Perseverance* rover drives at an unprecedented rate on Mars. As of writing (Sol 960), she has driven 22,980 m, which far exceeds the distance traversed by previous rovers over the same time span (7,345 m for *Spirit*, 10,004 km for *Opportunity*, and 10,564 m for *Curiosity* (Rankin, et al. 2020) on Sol 960). Perhaps even more remarkably, *Perseverance* drove ~88.7% of the distance autonomously using the *Enhanced AutoNav (ENav)* capability (as of Sol 960), while *Spirit*, *Opportunity*, and *Curiosity* drove 23.6%, 5.4%, and 6.1%, respectively, with autonomous driving (Verma, et al. 2023). The enhancement of the autonomous driving capability was required because Jezero Crater, the landing site of *Perseverance*, was known to have substantially higher rock density and slope from the high-resolution images of the HiRISE camera on Mars Reconnaissance Orbiter (Ono, Rothrock, et al. 2016).

The development and V&V of the advanced autonomous driving capability of *Perseverance* was enabled by existing environmental knowledge obtained by preceding missions. For example, ENav was required to drive the rover at the rate of 100 m/hr on benign terrain and 86 m/hr on complex terrain to achieve the mission objectives, where terrain is defined as benign if the slope is less than or equal to 15 degrees and the rock abundance is less than or equal to 7% CFA (cumulative fraction of area)<sup>3</sup>. Since the requirement was written in a way that is conditional on environmental parameters (slope and rock density), the V&V of ENav against the requirement needed to depend on the localized knowledge of these parameters. Using the 25 cm resolution imagery from HiRISE, a slope map at 1 m resolution and a rock density map at 30 m resolution were created. A Monte-Carlo simulation was then run with thousands of samples over the distribution of the landing point, and a path to the science goals from each sample of the landing point was simulated using the existing knowledge of the terrain traversability (Ono, Rothrock, et al. 2016). The Monte-Carlo simulation produced the statistics of slope and rock density. Combined with the digital elevation model (DEM), another Monte-Carlo simulation was run, in which the ENav path planner simulated more than 1,000 drives and verified that the driving speed requirements were statistically satisfied (Toupet, et al. 2020). Such a rigorous V&V process was impossible with the complete coverage of the landing site with high-resolution orbital imagery.

For another example, ENav was required to be robust to slips. Since the mission was going to involve climbing up a high slope at the edge of the delta in Jezero Crater, guaranteeing the vehicle's safety from slip hazards was critical. For this purpose, ENav sets bounding boxes around each wheel and runs conservative collision checking (Otsu, et al. 2019) at every 25 cm of drive such that any wheel slip within the bounding boxes is accommodated. One of the challenges during the development was finding the right size of the bounding boxes because ENav becomes overly conservative if they were too large but could result in critical failure if they were too small. The team relied on historical slip data from previous rover missions to address this challenge. Specifically, they used the data set containing *all* the observed slips that occurred during nominal drives of the preceding rover, *Curiosity*, from her landing in 2012 till the time of the ENav development around 2018 and set the bounding box sizes to accommodate them.

### B. The coring drill of the Mars 2020 *Perseverance* Rover

One of the top-level objectives of the Mars 2020 Rover Mission is to acquire and cache carefully selected rock samples for potential return to Earth. For this purpose, the sampling and caching system (SCS) was designed to core rock samples, document and seal the sample tubes, store them inside the rover body, and drop them on the ground at a sample depot. SCS is a highly complex system consisting of the Robotic Arm (RA), the Turret and Corer, and the Adaptive Caching Assembly (ACA). In particular, the development of the coring drill was challenging because it would directly interact with the external environment (i.e., Martian rocks) with unknown characteristics. The development and testing approach was to rely on the extrapolation from the environmental knowledge acquired from prior missions.

For example, the extensive Qualification Model Dirty Testing (QMDT) of the coring drill was conducted using six geo-analog rock types shown in Figure 2: Bishop Tuff Intermediate (BTI), Napa Basaltic Sandstone (NBS), Kramer Massive Mudstone (KMM), Old Dutch Pumice (ODP), China Ranch Gypsum (CRG), and Uniform Saddleback Basalt (USB) (Moeller, et al. 2021) (Farley 2015), which were carefully selected by the JPL Geo-Analogs team to represent a diverse and realistic variety of test articles that would mimic material characteristics of those

<sup>3</sup> To put it in perspective, *Curiosity*'s average autonomous driving speed was 11.6 m/hr (Verma, et al. 2023).

potentially found during the Mars 2020 mission (Chu, Brown and Kriechbaum 2017). The selection was heavily informed by prior missions. For example, USB is a basalt sourced from the Tertiary Tropico Group in the western Mojave Desert, chosen for its inert hygroscopic characteristics and its physical and chemical characteristics that resemble basalt rocks observed by Mars Pathfinder and the two Mars Exploration Rovers (Peters, et al. 2008). Over 700 coring tests were performed on the six rock types (ODP was dropped in the later test campaign) to meet the following two requirements:

- 1) Acquire average rock core masses of greater than or equal to 15 g, and less than or equal to 10% of the rock cores that are less than 10 g
- 2) No greater than 20% by mass of the core in pieces with the largest dimension less than or equal to 2 mm (effectively “powder”) and no less than 70% by mass of the core in pieces with the largest dimension greater than or equal to 10 mm.

The second requirement is to ensure that most of the cored rock sample is not broken into powdery pieces. The SCS performed “very well” and met these requirements for the selected geo-analog rocks (Moeller, et al. 2021).

The limitation of this test approach was exposed at the very first coring attempt on Mars by *Perseverance*. On August 6, 2021, the rover successfully executed the automated sampling process at Polygon Valley. However, the CacheCam image, which captures the interior of the sample tube before it was sealed, showed no rocks (Figure 3). It



**Figure 2. Examples of rock cores of the five rock types collected in the Qualification Model Dirty Testing.** The tests of the coring drill were performed only on six geo-analog rock types, which were later downselected to five. From left to right: Kramer Massive Mudstone (KMM), China Ranch Gypsum (CRG), Bishop Tuff Intermediate (BTI), Napa Basaltic Sandstone (NBS), and Uniform Saddleback Basalt (USB). Image from (Moeller, et al. 2021). Credit: NASA/JPL-Caltech.

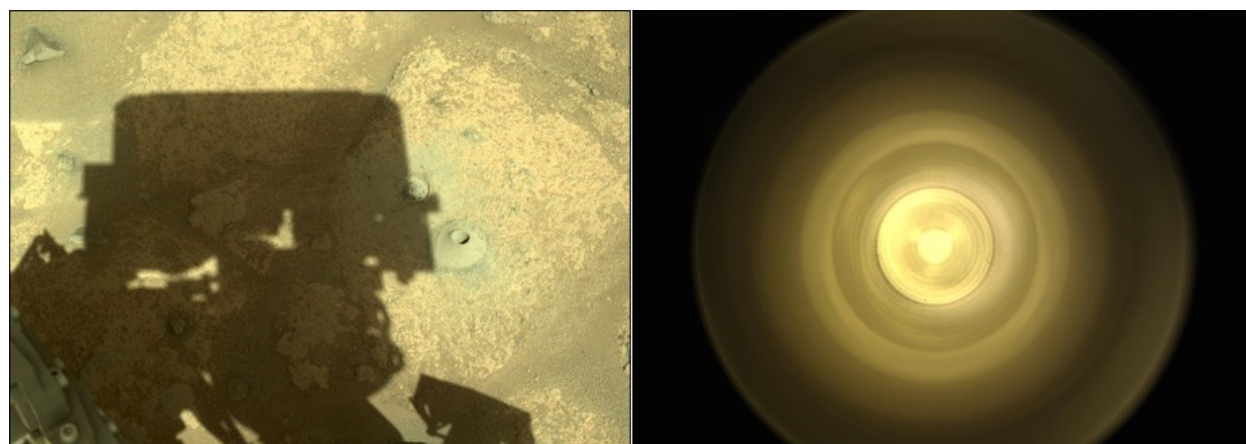


**Figure 3. *Perseverance*'s first sampling attempt at Polygon Valley on August 6, 2021.** The rover's coring drill successfully drilled the target rock (left), but no rock sample was found in the interior of the sample tube, as shown in the CacheCam image (right). It turned out that the rock was unexpectedly soft, and it crumbled and fell out of the tube. Such a rock was not represented in the six rock types, selected based on the experiences from past missions, on which the drill was tested on the ground before the launch. Credit: NASA/JPL-Caltech.

turned out that the rock was particularly soft, and it crumbled to powder during coring and fell off from the tube (NASA/JPL-Caltech 2023). The empty sample, named Roubion, was later repurposed as an atmospheric sample. The characteristics of the Roubion rock were not represented in the six rock types used in the coring tests. This result was unexpected because the drilling by *Curiosity* did not result in an empty sample. Based on this experience, the ground operation team changed the sampling procedure such that the rock sample is less likely to fall from the tube. All the following sampling attempts were successful. Therefore, this example also demonstrates the effectiveness of on-site adaptivity to deal with environmental uncertainty, although the adaptation was performed with the ground in the loop.

### C. Mobility and Manipulation System of the Sample Recovery Helicopters

The current baseline mission architecture of the planned Mars Sample Return Mission campaign (which is currently under high-level review) includes two small helicopters called *Sample Recovery Helicopters* or *SRH*, which would serve as a backup method for retrieving the sample tubes. The *Perseverance* rover collected two samples at each sampling site (except for the atmospheric sample at Polygon Valley and a singular sample from Kukaklek) during the first 1.5 years on Mars. Before the rover ventured to the top of the delta, she left one of each pair (eight sample tubes in total), as well as the atmospheric sample, at the carefully selected sample depot site called Three Forks while carrying the rest of the samples with her. In a nominal scenario where *Perseverance* is still operational when the Sample Retrieval Lander (SRL) arrives on Mars, the rover would hand the samples to SRL directly. Otherwise, the two SRHs, dispatched from SRL, would retrieve the nine backup samples left at Three Forks one by one and deliver them to SRL. The Three Forks depot site was selected because it was very flat, devoid of large rocks and high slopes.

Each SRH is a small (~3 kg) “flying car,” which combines the aerial mobility inherited from Mars Helicopter *Ingenuity* with the ground mobility enabled by four small wheels at the end of the landing legs and a 3 DOF light-weight robotic arm for picking up the sample tube (Mier-Hicks, et al. 2023). At each tube transport run, an SRH would fly from SRL and land about 2 m away from a tube. Then she would autonomously drive on the ground and park right in front of the tube to put the tube within the highly constrained workspace of the arm (required precision:  $\pm 1.5$  cm in X,  $\pm 4$  cm in Y, and  $\pm 5$  deg in heading). On the return flight, she would land in the “helipad” 10 m away from SRL and drive up to the workspace of the SRL arm to deliver the sample tube. Each SRH is required to repeat this cycle every 4 Martian Sols.

One of the greatest challenges of SRHs is to reliably perform such highly complex robotic tasks with a minimalistic hardware design due to the very tight mass budget. Therefore, the team took a design approach that fully exploited the intricately detailed environmental knowledge of the Three Forks depot site brought by the *Perseverance* rover. For example, using the documentation images taken at each dropped tube and in the SRL landing circle, the team identified rocks on the order of centimeters tall and determined that the SRH ground mobility system is only required to go over 3 cm high rocks to achieve >99% confidence of successfully driving up to the tubes to pick them up, and driving up to SRL to drop them off. This knowledge allowed the team to minimize the diameter of the wheel to conserve mass and fit in the tight space allocated for launch. The development of the autonomous driving capability was also informed by the knowledge of rock size and distribution (Reid, Bartlett, et al. 2024). The team also exploited the knowledge of the size and the relative location of all the rocks taller than ~3 mm within a certain distance around each tube (Figure 4) to validate the minimalistic gripper design. For another example, the team determined that it is sufficient to require SRH to handle only up to 5.5-degree slopes based on the slope map at a 50 cm resolution created from the high-resolution stereo images taken by *Perseverance*. This highly optimized design approach, which narrowly targets a specific, well-documented site on Mars, is only made possible by the serial nature of the Mars exploration campaign, where the spacecraft is designed based on the environmental knowledge acquired by prior missions.

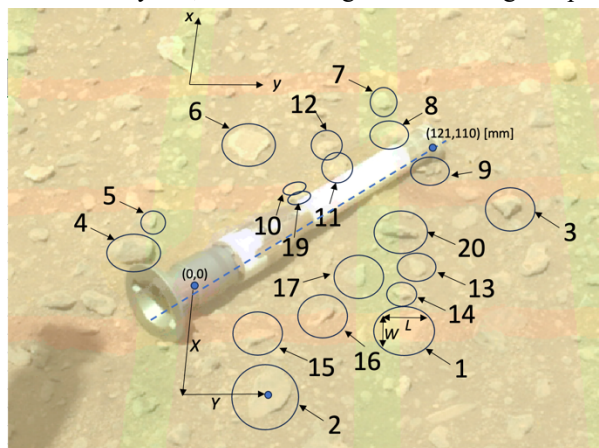


**Figure 4** An example of rocks on the order of millimeters high identified around one of the sample tubes in an image taken by Mars rover *Perseverance* for gripper validation of the Sample Recovery Helicopter (SRH). This exemplifies the dependence on the highly detailed environmental knowledge brought by preceding missions for the development of complex robotic capabilities. Credit: NASA/JPL-Caltech

#### D. Limiting factors for the current incremental exploration paradigm

The complex robotic capabilities in the Mars missions, such as the ones described above, depended on detailed environmental knowledge from prior missions because, in the conventional paradigm, the robot's behaviors must be designed and tested before the launch. The same limitation applies to combined orbiter-lander missions, such as the Viking mission in the past and the Enceladus Orbilander mission concept recommended by the Planetary Science and Astrobiology Decadal Survey 2023-2032 (National Academies of Sciences, Engineering, and Medicine 2022) in which an orbiter and a lander are launched at the same time because the lander (and a potential rover on it) must be designed before the high-resolution images from the orbiter become available.

A key observation is that, in most cases, the primary source of environmental uncertainty is the terrain for two reasons. First, surface robotic activities are often sensitive to the scale terrain features below the detectable limits from orbiters. Subsurface exploration would be even more challenging because orbital reconnaissance is impossible at any scale. Second, terramechanics, or the interaction between mechanical systems and soil, rocks, or ice, is highly unpredictable (e.g., wheel slip, drilling), in contrast to the almost-perfectly predictable orbital mechanics. Another key observation is the negative correlation between the complexity of robotic behavior and the level of environmental uncertainty that can be accommodated. For example, coring rocks, as described in Section II.B, is more sensitive to the physical properties of rocks than abrading them, as was done by *Spirit* and *Opportunity*. There are two approaches to circumvent these fundamental limitations. The first is to send a series of increasingly complex missions, in which the observations from earlier missions reduce the environmental uncertainty and inform the design of more sophisticated capabilities in the following missions. This is the current exploration paradigm shown in Figure 1-A. An underlying assumption in this paradigm is that the robotic behaviors are designed and fixed *before* the launch. If we can relax this assumption, an alternative paradigm becomes available, which will be discussed in the next section.

### III. New Paradigm: One-shot exploration with *in-situ* adaptation

Imagine you find yourself in a completely unknown place when you wake up, say, in the middle of a rainforest or a desert. You would carefully raise your head and look around to understand the situation. Then, you would take a few very cautious steps to learn more but avoid any close interaction with the environment. As you build up confidence in your understanding of the environment, you would finally dare to perform more complex behaviors that are deemed safe under the given situation, such as touching selected objects around you, picking up a rock or two, or moving over a longer distance with a gait that is suitable for the observed surface condition. In other words, you adapt your behaviors as you learn about the environment instead of replacing yourself with someone more suitable for the environment.

An adaptive robotic explorer can do the same, i.e., adapting the behavior *in situ* and incrementally elevating the level of behavioral complexity based on the environmental knowledge acquired by itself. As illustrated in Figure 1-B, it would land in a poorly characterized environment and observe the surroundings to reduce the environmental uncertainty. It would then adapt its behavior to perform relatively simple tasks, such as short-range/slow surface mobility and reconnaissance, to gain more environmental knowledge and further reduce uncertainty. Eventually the robot would make further adaptations to conduct complex robotic tasks such as long-range fast traverse, sample collection, and subsurface exploration. The key difference from the conventional paradigm is to design the robot for adaptivity over a wide range of environmental possibilities rather than designing it to narrowly constrained environmental conditions. In the remainder of this section, we will use three examples from existing research to illustrate how adaptive robots can overcome the existing limitations of the conventional paradigm. We will then discuss the key enabling technologies for the new adaptive exploration paradigm.

#### A. Sand trap experienced by Mars Rover Opportunity and EELS

In 2005, the Mars rover *Opportunity* became trapped in unexpectedly soft sand, as shown in Figure 5-Left. While high-resolution orbital reconnaissance provided detailed topographical knowledge of the terrain of Mars, the surface properties, such as softness, remained uncertain, particularly in the early phase of the Mars Exploration Rovers missions. The rover was not adaptive because it had a singular mode of mobility (i.e., driving); hence, what the ground operation could do was limited to spinning wheels in various ways. It took 39 sols (Martian days) to get the rover out of the sand trap. Later, the sister rover *Spirit* was also entrapped in sand, eventually ending her mission.

Compare this incident to one of the surface mobility tests of JPL's snake-like EELS robot, which will be detailed in Section IV, shown in Figure 5-Right. The robot dug into the sand and got stuck during a forward motion. But then the robot adapted its behavior by switching to a sidewinding gait, and it could easily get out of the sand trap by rolling sideways. As an analogy, animals typically have multiple gait patterns (e.g., locomotion modes of biological snake include lateral

undulation, sidewinding, concertina, arboreal, and rectilinear) and chooses the most suitable one for a given surface condition.



**Figure 5 Comparison of non-adaptive and adaptive robots. Left:** It took 39 sols for Mars rover Opportunity to escape from a sand trap in 2005 because a rover has a single mode of mobility (driving), and the only behavior the group could command was to rotate the wheels. **Right:** EELS is versatile, meaning it has multiple modes of mobility. When it got stuck in the sand when driving forward, it switched to a different sidewinding gait and could easily escape the sand trap by rolling sideways.

### B. Icy moon surface mobility with wheel-on-limb mobility

The surface topography of icy moons, such as Europa and Enceladus, is highly uncertain not only because of the lack of high-resolution orbital reconnaissance but also because of entirely different geomorphology from rocky, water-shaped surfaces, such as that of Earth and Mars. The surface geology of Enceladus is highly diverse and includes surface topographic variations with amplitudes of hundreds of meters (Thomas, et al. 2007). The current global maps of Enceladus from *Cassini* are typically at resolutions of 50 to 500 m/pixel (Bland, et al. 2018), much larger than the footprint of the proposed Enceladus Orbilander concept, which is only a few square meters (MacKenzie, et al. 2021). In another example, (Hobley, et al. 2018) hypothesized blade-like structures, called penitentes, might form on the surface of Europa and rise to many meters in height, while an experimental study by (Hand, Berisford, et al. 2020) suggests the existence of giant penitentes on Europa is unlikely. While the upcoming Europa Clipper mission will substantially improve the understanding of the Europa's surface through multiple flyby observations (Vance, et al. 2023) the coverage with high-resolution (4-m spatial scale) imagery will be limited, and sub-meter scale surface topography will remain largely unknown until the first landing mission.



**Figure 6 IceSimian traversing on extremely rough terrain in Devil's Golf Course, Death Valley (Reid, Paton, et al. 2020)**

(Reid, Paton, et al. 2020) demonstrated that wheel-on-limb mobility can cope with extremely rough terrain. They used the IceSimian robot, which has four fully actuated arms with wheels at the arm termini, as shown in Figure 6. This mechanical configuration allows a wide range of mobility modes, from regular wheel mobility with and without actively articulated suspension to more exotic gaits such as inchworming and wheel walking. As a result of the tests at Devil's Gold Course in Death Valley and on Matanuska Glacier in Alaska, they found that regular wheel mobility is more energy efficient on flat terrains, while inchworming is more resilient on high slopes (Reid, Merion-Griffith, et al. 2021). But perhaps more importantly, the robot's versatility allowed the operation team to *adapt* its mobility

behavior after the arrival at the test sites rather than pre-planning the mobility mode for preexisting environmental knowledge.

### C. Steep terrain mobility with an adaptive rover

One of the limitations of conventional wheeled rovers is the mobility on steep slopes with unconsolidated surfaces such as sand or Lunar regolith. Substantial backward slip could prevent the forward motion or make it highly energy inefficient at best. Lateral slip when driving in a cross-slope direction poses a risk of collision with obstacles. This limitation can be relaxed if a rover is adaptive to the environment. For example, (Bouton, et al. 2023) experimented with rovers that have extra actuated degrees of freedom and hence have multiple modes of mobility, such as “inchworming” or “push-pull” locomotion (Figure 7-left). They experimentally showed that conventional driving with passive suspension is the most energy efficient up to 20-degree slope on Lunar regolith simulant, while the load-adjusted squirming gait (Figure 7-right) can climb steeper slopes more efficiently. They also reported that unconventional locomotion gaits, such as circular wheel-walking (Figure 7-right), can reduce slip by 15-20%. Again, the point is the versatility of the robot, which allows the operator to select the best mobility mode for a given environment rather than pre-fixing the behavior based on limited environmental knowledge.

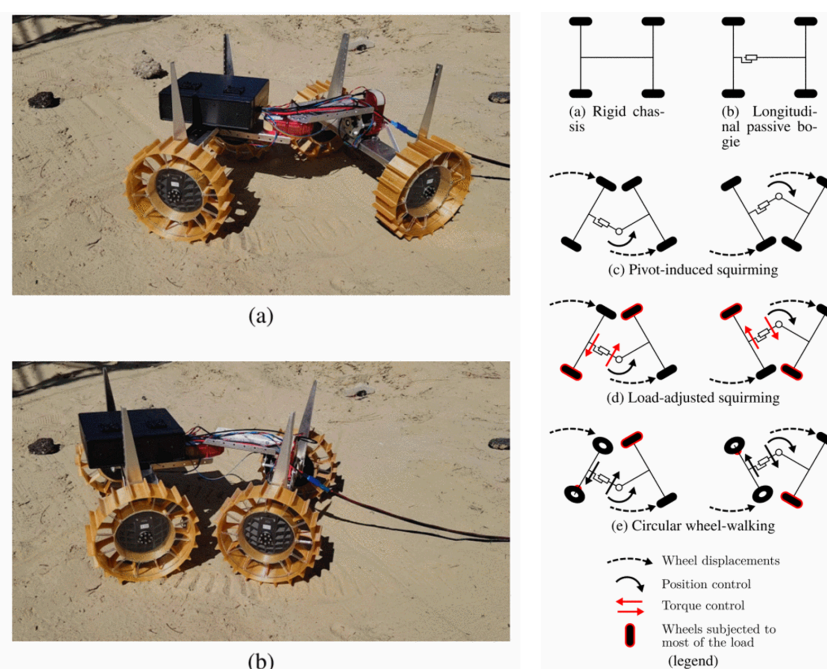


**Figure 7** The “Asterix” rover, which can locomote with multiple gait patterns due to the two extra DOFs in its body. Image excerpted from (Bouton, et al. 2023).

### D. Ingredients for Adaptive Robot: Versatility and Intelligence

Let’s find out the ingredients for making a robot adaptive through induction from these examples. We argue that they are versatile hardware and intelligent software.

#### Versatile Hardware: Redundant DOFs and sensing modalities

The essential feature to enable adaptation is the multiplicity of possible behaviors, or versatility. This, in turn, requires redundant degrees of freedom (DOFs). This sharply contrasts with the conventional paradigm that typically employs the simplest possible mechanical design to satisfy a given set of requirements, which are written based on narrowly constrained environmental/operational conditions. For example, it requires 6 DOFs for an arm to place the end effector at a desired 3D position at any angle. The robotic arm of the *Perseverance* rover only has 5 DOFs because the required tasks are indifferent to the roll angle of the turret at the end of the arm. In contrast, a human arm has 7 DOFs. This one extra DOF allows humans to improvise a wide range of the ways to use arms (e.g., a parent holding a baby in an arm and a cell phone on the shoulder while taking a note using the other arm, or a waitress in Oktoberfest who transports 13 beer glasses at the same time (Luyken 2023)). Similarly, in the conventional paradigm, robots are designed to have just enough sensing capabilities to satisfy prescribed requirements. Having redundant sensing modalities would be crucial for robots to be adaptive. In particular, many

robots lack proprioception, which is known to play a central role in animal locomotion (Tuthill and Azim 2018). Versatility is often obtained at the cost of efficiency. For example, the most energy-efficient human transportation is a bicycle, which has only 3 DOFs but only consumes about one-third of the energy of walking the same distance. In contrast, a human’s body has over 200 DOFs, which allows highly versatile mobility from walking and running to jumping, climbing, and swimming. In the new adaptive paradigm, robot hardware should be designed for versatility instead of optimizing on a singular metric.

### **Intelligent Software: Overcoming Moravec’s Paradox**

Hans Moravec argued that logical reasoning tasks that are difficult for humans, such as numeric calculation or chess, are easy for AI, while sensorimotor and perception tasks that are seemingly easy for humans, such as grabbing a cup or inserting a screw into a hole, are difficult for robots (Moravec 1988). This observation, known as *Moravec’s Paradox*, is more evident on a high-DOF robot simply due to the challenge of controlling a complex system. For example, in the successful vertical mobility demonstration of EELS, which will be described in Section IV.E, the most difficult software aspect was the low-level feedback control to maintain the contact between the arms and the walls. For humans, it is an easy task to keep touching a wall. Therefore, by *intelligence*, we do not necessarily mean logical reasoning, which is typically the goal of classical AI. Instead, our emphasis is on *bodily intelligence*, which includes proprioceptive control for limb placement, locomotion with complex gaits, gait learning, gait selection, motion/path planning, and risk-aware behaviors, combined with situational awareness and the understanding of the environment through multiple channels of sensory data. To give one example, in the sand trap escape demo of EELS described in III-A, it was human operators who commanded to switch the mobility mode. On the surface of a distant planet, a robot must understand the situation (trapped in sand), understand the environmental condition (unconsolidated sand), identify the tactical goal (escape from the sand trap), and choose the optimal behavior for achieving the goal (side winding gait). Since it would be impractical to implement all the behavioral patterns for a high DOF robot before launch, a robot would have to synthesize new behaviors on-site to be fully adaptive. Humans and animals acquire new behaviors in multiple ways: trial and error or reinforcement learning (e.g., babies learning how to crawl/walk), supervised learning, and imitation learning. Sometimes, we improvise a new behavior without trial and error, guidance, or imitation, such as the triple-tasking parent of a baby mentioned above. Such improvisation is presumably performed through solving a model-based planning problem.

The following section presents our instantiation of a highly versatile and intelligent robot.

## **IV. EELS – A highly versatile and intelligent robotic explorer for Enceladus vents and beyond**

JPL has developed a snake-like robot called *Exobiology Extant Life Surveyor (EELS)* as an instantiation of a highly versatile and intelligent robot for enabling the new adaptive exploration paradigm. Three prototypes of EELS have been built and extensively tested in field environments, including Athabasca Glacier in Canada. This section presents a broad overview of our vision, prototypes, instrument, and test results while leaving the details for the three companion papers and other publications.

### **A. Vision: Enabling access to the subsurface ocean of icy moons**

Enabling access to the subsurface ocean of icy moons is a key target of robotic space exploration because it is arguably the most likely place where we might find evidence of extant alien life in the Solar System, if it is there (Hand 2020). There are two approaches often discussed for accessing the subsurface oceans or liquid reservoirs of icy moons. One is to melt through the ice crust, which is typically tens of km thick, using a cryobot (Zimmerman, Bonitz and Feldman 2001) (Hockman, et al. 2022), while the other is to send a small robot into a natural opening of the ice shell that has evidence linking it to the ocean. *Cassini* observations of Enceladus, a small icy moon of Saturn, revealed the existence of actively erupting vents, which are likely connected to its global subsurface ocean (Schenk, et al. 2018). Meanwhile, the detection of localized water vapor on Europa by the Hubble Space Telescope indicates the potential existence of similar vents on the Jovian icy moon (Sparks, et al. 2016) (Jia, et al. 2018). A previous study demonstrated that a robotic mission into an erupting vent is technically feasible except for an extreme case where the largest vent on Enceladus has a diameter of <10 cm (Ono, Karl, et al. 2018). *Cassini*’s observations suggest that there are >100 active vents on Enceladus (Porco, DiNino and Nimmo 2014). While we cannot completely eliminate the possibility that all of them are <10 cm, such a possibility would be rather unlikely, given the substantial mass flux (300 kg/s, recently confirmed with JWST observations to still be stable since *Cassini* (Villanueva, et al. 2023)). In the following study, we performed a mission architecture trade study to determine whether an implementable mission architecture exists. It considered alternatives in instrumentation, mobility systems, sampling strategies, landing location, and the number of spacecraft elements. As a result, we found that an Enceladus vent exploration mission is implementable within the

Flagship mission launch mass and cost constraints (Chodas, et al. 2023). The study also found that the main risk of the mission is environmental uncertainty, which resonates with the theme of this paper.

EELS was conceived to enable such a mission. As illustrated in the artist's concept in Figure 8, the robot would be deployed by a lander near an actively erupting vent (e.g., near one of the sulci of the South Polar Terrain of Enceladus) and slither on the surface to identify the most suitable entry point. It would then descend into the vent while firmly pushing the opposing walls to resist the dynamic pressure from the jet. If a clear interface between the gas and the liquid phases of the water exists (as in the hypotheses by (Kite and Rubin 2016) (Nakajima and Ingersoll 2016)), it should be located at a depth of about 10% thickness of the ice shell; in an alternative hypothesis where a liquid-gas mixture is propelled by the gas expansion (Mitchell, Rabinovitch, et al. 2023), EELS would only need to descend a few hundred meters to capture a fresh liquid sample (Chodas, et al. 2023). In either case, EELS would use in-situ instruments to search for biosignatures in the water sample and/or return the samples to the lander, which can accommodate larger instruments for detailed analysis.



**Figure 8. EELS Concept for enabling Enceladus subsurface ocean access.**

The application of EELS is not limited to icy moon exploration. For example, past Lunar orbiter and impact missions confirmed the existence of water ice trapped in craters with permanently shadowed regions (PSRs) (Laurence 2017). Retrieving the ice samples from Lunar PSR is of particular interest for both scientific investigation and in-situ resource utilization (ISRU) (Artemis III Science Definition Team 2020) (Brown, et al. 2022). However, the crater rim with a high slope (typically up to 20-30 degrees) with unconsolidated regolith, as well as unknown topography and the surface state of the interior due to the limitation in orbital reconnaissance, makes the access to the deep interior of PSR highly challenging for conventional robots. It is even more challenging for astronauts because of the extreme temperature of PSRs, as well as the restriction of their mobility to a slope less than 10 degrees for safety. The underground lava tubes on the Moon and Mars are another example of high-value targets that are challenging for conventional robots or astronauts. An adaptive robot such as EELS could enable the exploration of such destinations.

## **B. EELS Mechanical System Overview**

The versatility of EELS is sourced from its high degree-of-freedom (DOF) mechanical design. In a nutshell, its mobility system is a combination of snake mobility with the Archimedes screw. It consists of many semi-identical modules, each of which has four actuated degree-of-freedom (DOFs): two shape actuators, consisting of a "twist" joint that rotates axially and a "bend" joint that rotates about a lateral axis, and two actuated side screws. Right-handed and left-handed screws are placed alternatively such that they produce axial force when rotated in the opposite direction ("screw mode") or lateral force when rotated in the same direction ("wheel mode"), as shown in Figure 9. The modular design allows EELS to be configured with any number of modules. A 12-module EELS robot, for example, has 48 DOFs.

EELS has practically infinite ways of propelling itself by combining its rich DOFs in various ways. Broadly speaking, EELS's mobility modes are categorized into two types: shape-based and screw-based gaits. Shape-based gaits lock the side screws and only actuate the twist and bend joints to move. Biological snakes typically use four gait

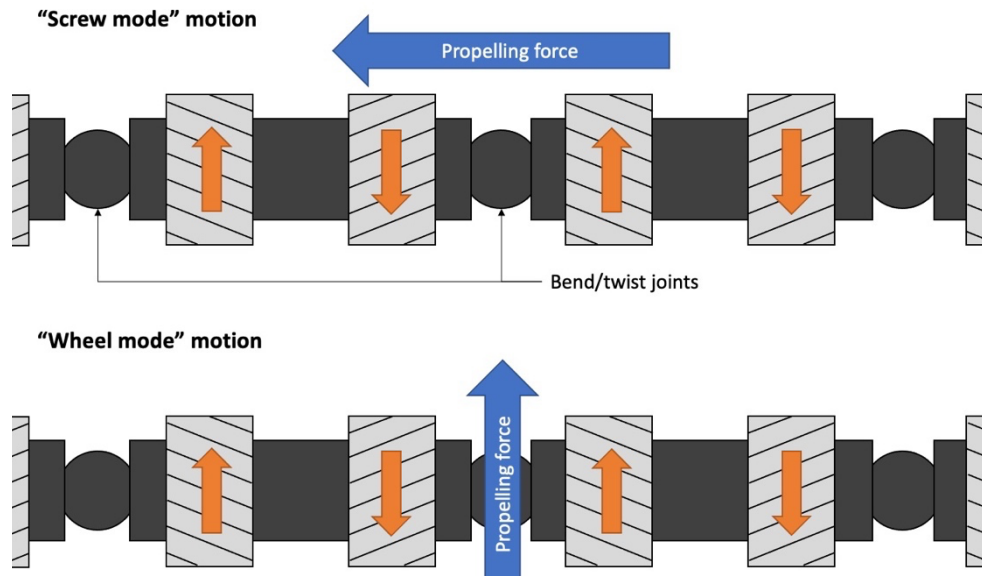


**Figure 10. The active skin propulsion system of EELS.** The independently actuated screws with alternating thread direction enables omnidirectional motion of the robot.

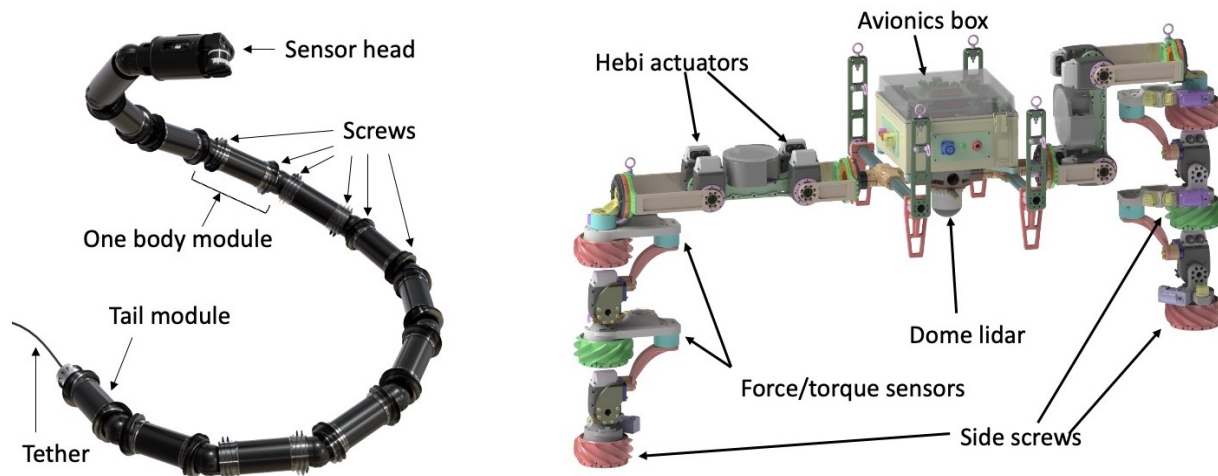


**Figure 9. The hardware configuration of the EELS 1.0 (left) and 1.5 (right) robots.** Although they look very different, they share the same hardware configuration: bend and twist joints between modules and the side screw for active skin propulsion. The two “arms” of EELS 1.5 represent the both ends of snake while the middle section is replaced by an avionics box.

patterns (rectilinear, lateral undulation, sidewinding, and concertina) (Jayne 2020), all of which are shape-based, obviously because snakes do not have side screws. Screw-based gaits use the side screws for propulsion, while the twist and bend joints are for conforming to the terrain. Screw-based gaits are further divided into two subcategories: the screw mode, in which the robot is propelled to the axial direction by counter-rotating the screws with the opposite thread handedness to cancel out the axial torque, and the wheel mode, in which the robot is propelled laterally by rotating all screws in the consistent direction, as depicted in Figure 8 3. For example, when EELS is straight and on the surface (as in Figure 8 top-left) or takes a helical shape in a vent (as in Figure 8 bottom-left), counter-rotating every other screw results in forward or backward motion (screw mode). When the robot is in a self-stabilizing pose and rotates all the screws in a consistent direction, it moves sideways on the surface or up and down in the crevasse (wheel mode). In practice, EELS can also use gaits that mix shape-based and screw-based mobility. It can also combine the screw mode and wheel mode for improved efficiency and robustness.

As of the writing of this paper, we have built three hardware prototypes for development and testing, which all use the common hardware configuration and the same software codebase: EELS 1.0, EELS 1.5, and Garden EELS.

The EELS 1.0 robot, shown in Figure 9-left, measures about 4.4 m long and weighs ~83 kg, consisting of 10 identical body modules that feature newly developed high power-density actuators (Georgiev 2023), a sensor head with a LiDAR, four pairs of cameras, and an IMU, and a tail module that houses the interface to the tether and another IMU. The mechanical and electronics systems are completely modularized such that they can be reconfigured with any number of modules. Although the robot demonstrated excellent performance in our field tests, as detailed in Section IV.E-F, it has several notable limitations. The two screws on each module are locked to counter-rotate at the same rate and driven by a single actuator and therefore did not support the “wheel mode” mobility (Figure 10-bottom) in its original design. After the realization of the value of the wheel mode mobility, the team removed one of the screws from each module and configured the remaining screws in alternating directions. This allowed substantially more versatile mobility but with a half number of screws. We drew a lesson from this experience: extra DOFs are essential for adaptivity. Another limitation of EELS 1.0 is the lack of force-torque sensing, which in turn restricts its ability of proprioceptive force/torque-feedback control, which turned out to be essential for vertical mobility. This gave us another lesson: extra sensing modalities are another essential recipe for adaptivity. These limitations will be addressed in the EELS 2.0 robot, which is currently under development.

EELS 1.5, shown in Figure 9-right, is an interim robot with commercial-off-the-shelf Hebi actuators that address the limitations of EELS 1.0 mentioned above. Since the completion of the planned EELS 2.0 robot, the ultimate successor to EELS 1.0, was not expected before the critical field test in Athabasca Glacier in 2023 described in Section IV.F, this ~50 kg robot was built to develop and test the vertical mobility capability quickly. Although the appearance is substantially different from EELS 1.0, it shares the fundamental mechanical features: shape and twist DOFs between each module and the side screws for active skin propulsion. The two “arms” of the robot represent both ends of the snake robot, while the middle modules are replaced by an avionics box as they are not necessary for the vertical mobility tests. Unlike EELS 1.0, it has only one screw per module. Force/torque sensors are inserted between the modules, and the actuators also provide joint torque sensing. EELS 1.5 successfully demonstrated vertical mobility in natural glacial holes, as detailed in Section IV.F.

Garden EELS (Figure 11) is a small experimental robot that only weighs ~4.5 kg, consisting of a series of DYANMIXEL actuators with no active skin propulsion. It serves two purposes. The first is to be a proof-of-concept for a smaller-scale portable EELS robot, and the second is to develop and test experimental shape-based gaits, such as reinforcement learning-based gaits.

More details of EELS hardware and the active skin propulsion are reported in the companion papers, (Gildner, et al. 2024) and (Marteau, et al. 2024), respectively. The hardware design is presented in (Georgiev, Pailevanian, et al. 2024) while (Georgiev 2023) details the actuator design and characterization.

In addition to hardware testbeds, we developed a physics-based simulator using JPL’s Dynamics Algorithms for Real-Time Simulation (DARTS) software framework (Jain 2019) to model EELS 1.0 and 1.5 in simulation. The so-called EELS-DARTS software simulates the full multibody dynamics of the robot and includes models for screw-terrain contact forces. Particularly with EELS 1.5, we also added force-torque sensing models, allowing us to close the loop with proprioceptive control in sim. By modifying external environmental factors such as gravity and terrain, as well as initial robot placement, we quickly prototyped control algorithms for many traversal scenarios before testing them on hardware (Figure 12).



Figure 11. The “Garden EELS” robot.

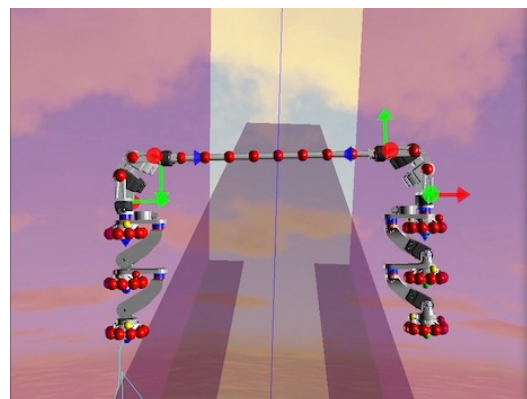


Figure 12. The EELS-DARTS simulator demonstrating vertical mobility of EELS 1.5 between parallel walls.

### C. EELS onboard intelligence for adaptivity: NEO Autonomy

All the EELS robots mentioned above are driven by a novel autonomy framework called *NEO* (Thakker, Paton, et al. 2024). Unlike conventional onboard software designed for satisfying prescribed requirements, *NEO* is designed for in-situ adaptivity at architectural and functional aspects.

As for the architectural aspect, *NEO* has behavior managers that allow flexible change in behaviors at every level of abstraction in the planning and control stack, as shown in Figure 13. In *NEO*, every robotic behavior is implemented as a library, shown as dashed boxes in the figure, which is activated or deactivated by its behavior manager. At the top level, the gait manager specifies the overall behavioral mode, such as surface and subsurface mobility; at the middle level, the local planner manager selects the gait and the corresponding motion planning algorithm; finally, at the lowest level, the controller manager activates a set of control behaviors that are needed for the current gait. This architecture enables seamless switching between behavioral patterns and accommodates additions of new behaviors without changing the overall architecture or requiring new software modules.

As for the functional aspect, *NEO* features a number of algorithmic capabilities that are needed for adaptation at every level in the stack. For instance, as explained in Section III and Figure 1, an adaptive robot in the new paradigm needs to change its behavior depending on the level of environmental uncertainty. This requires reasoning based on risk, i.e., trading off between performance and the risk the system is willing to take. For a simple example, a risk-sensitive human would walk slowly and cautiously with substantial safety margins in an uncertain environment (e.g., an unpaved mountain trail), while s/he would feel comfortable moving swiftly under less uncertainty (e.g., a paved sidewalk in a familiar place). We implemented a risk-aware planner that co-optimizes high-level actions and motion plans in consideration of risks and contingencies (Vaquero, et al. n.d.) (Daddi, et al. n.d.). At a lower level, controlling high-DOF hardware is a challenging task, particularly on highly undulating terrains or vertical walls. Over the course of development, we realized that proprioceptive control, which uses the sense of self-movement, force/torque, and body positions, is a key enabler. It is known that proprioceptive feedback plays critical role in human mobility at the unconscious level (Roden-Reynolds, et al. 2015) (Tuthill and Azim 2018). Using the joint torque sensing capability of the EELS 1.5 robot, we have implemented and successfully tested a simultaneous shape, contact, and force for vertical mobility that uses proprioceptive feedback. Finally, although most of the existing motion gaits for EELS were manually designed and implemented, we also experimented with reinforcement learning to demonstrate the self-discovery of new gaits that suit given environments. Using Nvidia’s Isaac Gym simulator, we spawned hundreds of simulated EELS robots initialized with random initial states and gait parameters and made them adapt the gait for efficient mobility (Figure 14). The resulting shape-based gait was successfully tested on the Garden EELS and EELS 1.0 robots (Figure 16-D). *NEO* also supports essential functions for robotic activities in extreme conditions, such as simultaneous localization and mapping (SLAM) in perceptually

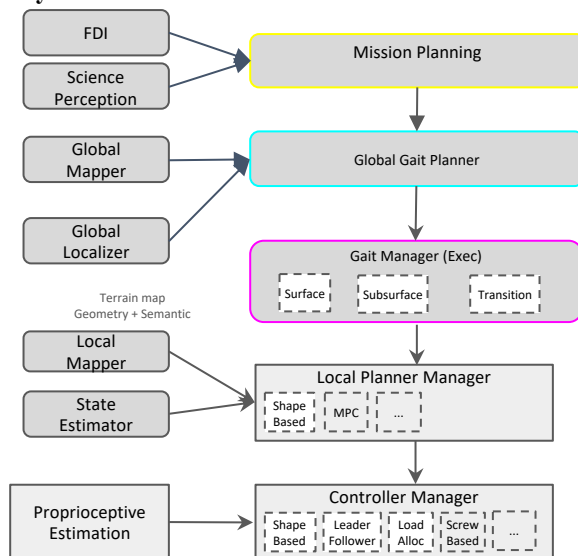


**Figure 13 Overall architecture of the NEO autonomy.** Behaviors are implemented as libraries (dashed boxes) while behavior managers at each level enables seamless switch between them.

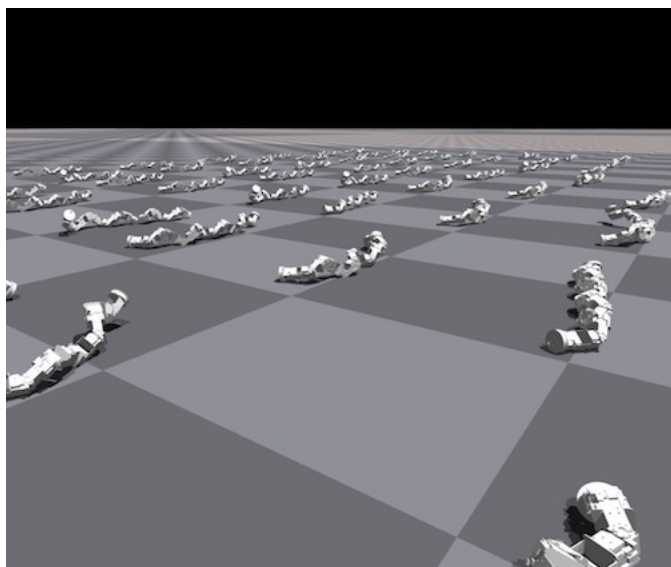


**Figure 14. Training of reinforcement learning-based gaits using NVIDIA’s Isaac Sim**

degraded environments (Talbot, et al. 2023) and sampling-based path/motion planning for a high-DOF system. More details of the NEO Autonomy are described in a companion paper (Thakker, Paton, et al. 2024) as well as in our previous publications (Thakker, Paton, et al. 2023).

#### D. Science instruments

Although the emphasis of the ongoing project is on autonomous versatile mobility, we also worked with the science community to develop two instruments to demonstrate that EELS has the ability to accommodate relevant scientific instrumentation. The first one is a capillary electrophoresis (CE) instrument, which showcases the ability of EELS to perform on-board analysis, while the second is the deployment of the *CryoEgg* sensor package to showcase the capability of EELS to be used as an instrument delivery platform for targeted drop-off of remote instruments or probes.

*Capillary Electrophoresis (CE) Instrument* – This instrument, designed to fit within a single EELS module (Figure 15-left), employs capillary electrophoresis with capacitively coupled contactless conductivity detection (CE-C<sup>4</sup>D) to identify and quantify cations and anions in liquid water samples, which is essential for assessing the habitability of icy moon oceans (Drevinskas, et al. 2023). We also note that these measurements were identified by subject matter experts as important for glaciology and cryosphere studies, enabling EELS measurements to contribute to Earth science goals and objectives, such as the evolution of physicochemical properties of glacial rivers. Equipped with two C<sup>4</sup>D detectors, it simultaneously analyzes both negatively and positively charged species. This cylinder-shaped tool, with a 10-cm diameter and 32-cm length, is a modification of a prior underwater CE design (Drevinskas, Mora, et al. 2023). The CE-C<sup>4</sup>D is encased in a watertight housing with five ports: (1) sampling, (2) internal standard, (3) background electrolyte (BGE) supply, (4) waste removal, and (5) auxiliary. Two gravity-independent high voltage reservoirs ensure its operation in any position or during motion (T. Drevinskas, A. Noell, et al. 2023). In its tested configuration, the instrument accommodates 25 mL of BGE, 25 mL of water for rinsing, and 50 mL for waste. Additionally, it features a pneumatics and liquid processing module for solution delivery, dilution, spiking, and fluidic line pressurization and purging. All requisite liquids are delivered to the CE module, which houses separation capillaries, detectors, a high-voltage power supply, and an injection valve. This module executes the analytical process, encompassing sample separation and compound detection. The instrument was successfully tested in field environments at Athabasca Glacier, including while fully immersed. The results of the experiments will be reported in upcoming publications.

*Cryoegg Instrument* – The Cryoegg is a wireless sensor package designed to explore subglacial systems (Prior-Jones, Bagshaw and et al. 2017). Its spherical form means that it can fit inside one of the EELS modules to allow autonomous release in a desired en- or subglacial location (Figure 15-right). EELS is capable of deploying Cryoegg into a sub-surface channel to record the temperature, pressure and electrical conductivity of subglacial water over extended (seasonal to annual) timescales. Data are returned from the egg to the surface via radio and recorded by a satellite-linked, solar-powered transceiver. Work is currently underway to design a module that can integrate and release a Cryoegg in an englacial conduit.

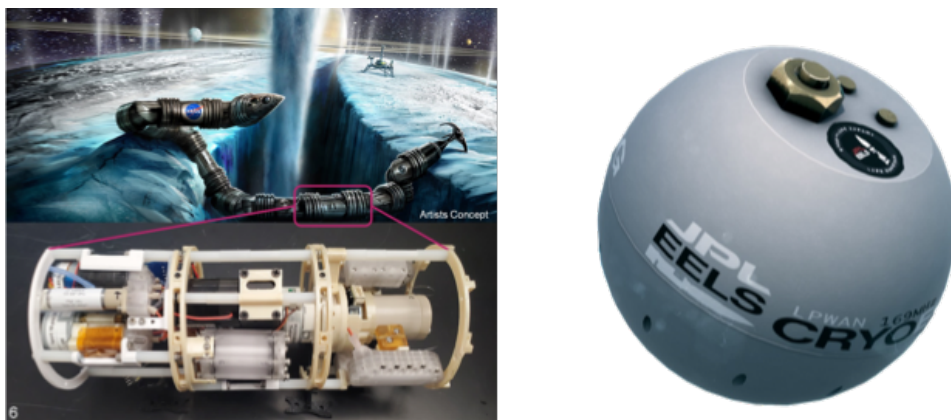


**Figure 15** EELS instruments. **Left:** The prototype of a capillary electrophoresis instrument that fits within one EELS module. **Right:** Cryoegg sensor package for monitoring the subglacial environment.

#### E. Versatile mobility of EELS

The high DOF design of EELS hardware and the flexible NEO Autonomy framework enabled a wide range of mobility modes, which in turn allowed the robot to be used in a wide range of environments. This subsection describes a subset of mobility modes of the EELS robots out of numerous possibilities.

*Leader-follower gait* – This screw-based gait for surface mobility locomotes the robot like a train, where all the modules follow a prescribed path, as shown in Figure 16-A. The robot is axially propelled by the screws while the shape actuators are controlled such that each module follows the trajectory of the preceding module. This gait is suitable for passing through a tight gap between obstacles. One of the advantages of the leader-follower gait is that it reduces the motion planning problem to a single tractable curve. For this reason, it is currently used as the primary gait for autonomous surface mobility. This gait has been tested on the EELS 1.0 robot in various field environments.

*Constant-shape gaits* – This class of screw-based gaits keeps the robot in a constant shape and executes the commanded two-dimensional motion, as shown in Figure 16-(B). At the core of this gait implementation is a screw velocity allocator, which takes the commanded motion and the current robot shape as inputs and translates them to the rotational velocity of every screw. Although we mostly use this gait with a pre-fixed shape for simplicity, the robot

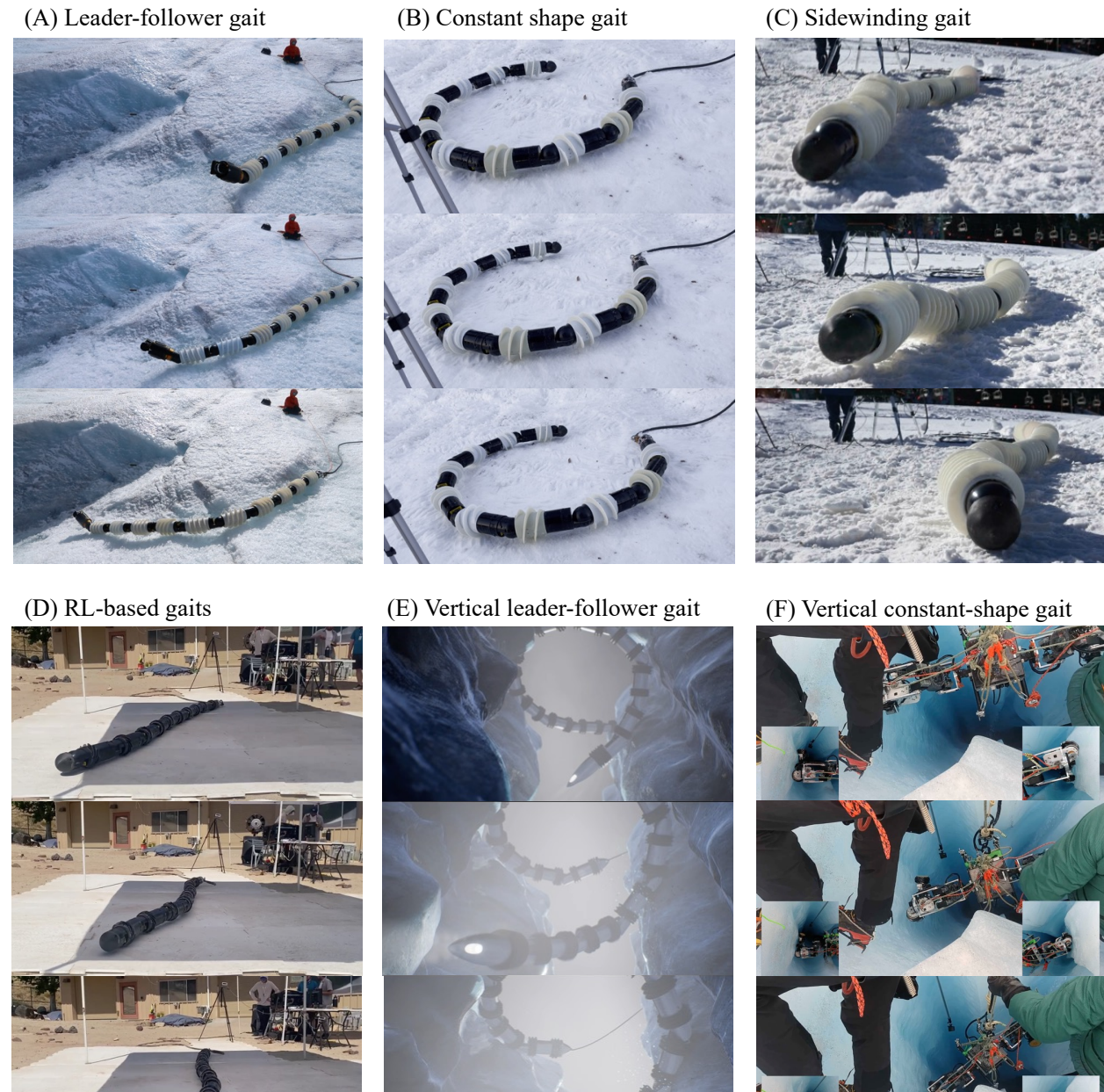


Figure 16 A subset of the mobility gaits of EELS

can change the shape while in motion. Constant-shape gaits are usually used to manually control the robot with a joystick because of its intuitiveness of the motion. This gait has been tested on the EELS 1.0 robot in various field environments.

*Sidewinding gait* – Inspired by a locomotion mode biological snakes use to move across loose or slippery substrates, this shape-based gait locks the screws and moves the joints in a sinusoidal pattern to move to the lateral direction, as shown in Figure 16-(C). Compared to screw-based gaits, it is more robust to terrain undulations, particularly on unconsolidated surfaces such as regolith or snow. This gait has been tested on EELS 1.0 in various field environments.

*Reinforcement learning-based gaits* – The three gaits mentioned above were directly implemented by human engineers. However, a high-DOF unconventional robot such as EELS can move in a highly unintuitive way beyond human imagination. One way to exploit the unexplored potential is to let the robot discover gaits by itself through trial and error using reinforcement learning (RL) (Figure 16-(D) shows an example that exhibits rotational motion only using shape-based actuators. RL can also tune existing gaits or even discover new ones in a new environment without humans in the loop. This gait has been tested on EELS 1.0 and Garden EELS robots in lab environments.

*Vertical leader-follower gait* – This is an extension of the leader-follower gait to a three-dimensional space, where every module follows a 3-D curve while the robot expands to push the walls for supporting its own weight or resisting the dynamic pressure from an upward jet. This gait is particularly suitable for descending or ascending in a cylindrical conduit with a spiral trajectory, as in Figure 16-(E). We implemented this gait with a spiral trajectory for an earlier prototype version that preceded EELS 1.0 and demonstrated vertical mobility in a cylinder. We did not implement this gait for EELS 1.0 or 1.5 in favor of the vertical constant-shape gaits explained below.

*Vertical constant-shape gaits* – This is a three-dimensional extension of the constant-shape gaits. We extensively explored these gait patterns for moving vertically between two parallel walls. In this particular use case, EELS bends itself in a “U” or “Z” shape and uses both ends to push the two walls against each other to support its own weight or resisting dynamic pressure while using the side screws for moving to a desired direction. We implemented many variations of this class of gaits named after the shape of alphabetical letters, such as “U,” “N,” “Z,” and “J,” and tested both in a walk-in freezer and a natural icy hole on Athabasca Glacier. The “J” variant was eventually used for the successful vertical mobility test in Athabasca Glacier, shown in Figure 16-(F).

Obviously, there are many other gaits that we have yet to explore or even imagine. Compared to a conventional vehicle with a singular mobility mode, such as the existing Mars rovers, this multiplicity of mobility modes enables the robot to adapt to a wide range of environmental possibilities.

## F. EELS lab and field tests

We extensively tested EELS robots on a wide range of environments, as summarized in Table 1. EELS robots have successfully driven on multiple surface types, including sand (JPL’s Mars Yard), ice (Athabasca Glacier, Pasadena Ice Rink, Table Mountain Observatory), and snow (Big Bear Ski Resort, Table Mountain Observatory). Some notable achievements include:

- Regolith mobility up to ~20-degree slope in JPL’s Mars Yard with EELS 1.0 using all types of mobility gaits (Figure 17-A)
- Autonomous ascent of a ~35-degree, snow-covered slope in Table Mountain Observatory with EELS 1.0 using the leader-follower gait (Figure 17-C)
- Autonomous positive and negative obstacle avoidance in the lab, JPL’s Mars Yard, Big Bear Ski Resort, and Athabasca Glacier with EELS 1.0 using the leader-follower gait (Figure 17-D)
- Semi-autonomous descent into and ascent from a ~2 m deep ice channel in Athabasca Glacier using EELS 1.0 using various surface mobility gaits (Paton, et al. 2024) (Figure 16-A, Figure 17-E)
- Autonomous ~1.5 m *vertical* descent in an icy hole (moulin) in Athabasca Glacier with EELS 1.5 using the vertical constant-shape gait (Paton, et al. 2024) (Figure 17-F)

The highlight of the test campaign was a 3-week long field trip to Athabasca Glacier in Alberta, Canada. We have conducted five surface mobility tests at three locations with slopes and undulations using EELS 1.0, seven vertical mobility tests at three moulins (vertical ice holes) using EELS 1.5, five in-situ, fully-autonomous analyses of glacial water with the CE instruments described in Section IV-D, screw mobility experiments (Marteau, et al. 2024), and collection of 3-D lidar scans at many locations. The details of the field trip are presented in (Paton, et al. 2024). Note that all the experiments in the diverse set of environments were made using only two robots (EELS 1.0 and 1.5) that share the common mechanical configuration and are driven by the same code base.

**Table 1 Summary of the lab and field tests of EELS**

Test venue	Date	Tested environment	Tested behaviors
JPL’s Mars Yard	Oct, 2022 – Jul, 2023	Sandy surface; up to ~20-degree slope.	All types of surface mobility gaits with EELS 1.0 (Figure 5, Figure 17-A)
Pasadena Ice Rink	Jul 13, 2022	Icy level surface; up to ~10 cm terrain undulation	Leader-follower and constant-shape gaits with EELS 1.0 (Figure 17-B)
Athabasca Glacier (Talbot, et al. 2023)	Sep 12-15, 2022	Icy vertical holes (moulins)	3D Perception with EELS 1.0 sensor head
Table Mountain Observatory	Dec 22, 2022	Unconsolidated (snow) and consolidated (ice) surfaces up to ~35-degree slope	Open-loop leader-follower and constant-shape gaits; slope mobility on snow with EELS 1.0 (Figure 17-C)
Big Bear Ski Resort	Feb 14-15, 2022	Unconsolidated (snow) surface with terrain undulations and slopes	Closed-loop leader-follower gait and open-loop constant-shape and sidewinding gaits with EELS 1.0 (Figure 16-C)
JPL’s walk-in freezer	May-Sep 2023	Two parallel ice walls with undulation	Vertical constant-shape gaits with closed-loop proprioceptive control with EELS 1.5
Athabasca Glacier (Paton, et al. 2024)	Sep 10-30, 2023	Unconsolidated (snow) and consolidated (ice) surfaces with up two ~2 m height difference	Closed-loop leader-follower gait and open-loop constant-shape and sidewinding gaits with EELS 1.0 (Figure 16-A, Figure 17-E)
		Icy vertical holes (moulins)	Vertical constant-shape gaits with closed-loop proprioceptive control with EELS 1.5 (Figure 16-F, Figure 17-F)

**G. Additional adaptive behaviors of EELS**

In addition to adaptive mobility behaviors above, we implemented a couple of additional non-mobility behaviors. For example, Figure 18-left shows a “head up” behavior for increasing the range of onboard perception. Since the height of the perception head is low during the surface motion, EELS often suffer from limited range and resolution of the local map used for obstacle avoidance. We implemented a risk-aware behavior in which the robot autonomously stops the traverse when the map quality is insufficient and raises its head to scan the environment (Vaquero, et al. n.d.) (Daddi, et al. n.d.). For another example, Figure 18-right shows a manipulation behavior where EELS uses the tail end as a robot arm with a gripper attached to the tail section while the perception head is raised to map the manipulation target.

During the lab and field tests, we had a number of anecdotal cases, often unexpectedly, in which the adaptivity of EELS solved problems. For example:

- Escape from sand trap with sidewinding gait, as described in Section III-A and shown in Figure 5.
- Gradual degradation with a lost module. During the field test in Table Mountain Observatory, the side screw of one of the modules stopped working due to a mechanical issue. The robot remained operational and mobile with the remaining nine modules (after manually removing a screw from the malfunctioned module), and we successfully completed the planned tests (Figure 17-C). This example demonstrates that modularity is another recipe for adaptivity.
- On-site gait adaptation. In one of the surface mobility tests at Athabasca Glacier, the EELS 1.0 robot experienced substantial slip while climbing up the icy slope of an ice channel. The robot operator tuned the shape parameters to better comply with the terrain undulation and successfully climbed up the slope.
- Quick gait iteration. Over the course of the development of the vertical constant-shape gait in JPL’s walk-in freezer, the team quickly iterated over multiple variations of the shape (e.g., “U,” “Z,” “J,” etc.) to enhance the stability of the robot between the two vertical ice walls.

These early successes demonstrate the potential of the robot to adapt to the environment *after* landing in an unvisited world. However, we note that the adaptation in these examples was performed manually, including parameter tuning and software updates. Enabling autonomous adaption is our future work.

(A) Sandy slope, JPL's Mars Yard



(B) Icy surface, Pasadena Ice Rink



(C) Snow slope, Table Mountain Observatory



(D) Obstacle avoidance, ice simulant panels in the lab



(E) Undulating icy surface, Athabasca Glacier



(F) Vertical ice hole (moulin), Athabasca Glacier



**Figure 17 Adaptive mobility of JPL's EELS Robot in lab and field environments**



**Figure 18 Non-mobility behaviors of EELS. Left: "head up" behavior for increasing the range of onboard perception. Right: Manipulation behavior with a gripper at the tail section.**

## V. Conclusion: One small step toward the realization of the new exploration paradigm

We observed from several notable examples in the Mars 2020 and Mars Sample Missions that the development and V&V of complex robotic capabilities often depended on the detailed environmental knowledge brought by preceding missions (Section II). However, as NASA is looking to explore a multitude of more challenging and scientifically fascinating worlds, we will likely not enjoy the same luxury of sending many spacecraft to the same world due to the tight budgetary constraints, scarcity of flight opportunities, and the extensive cruise time to the Outer Solar System and beyond. We argued for a new robotic exploration paradigm, which replaces a series of incrementally sophisticated missions with a single-shot mission where a robot or a team of robots adapt its behavior *after* landing and incrementally elevates the level of behavioral complexity as it learns about the environment (Section III). After reviewing several existing robotic systems that are adaptive (Section III.A-C), we concluded that the key ingredients for adaptivity are hardware-level versatility and onboard intelligence that focuses on physical interaction with the environment (Section III.D). We introduced our instantiation of a highly versatile and intelligent robot, EELS, which is envisioned to enable access to the subsurface ocean of icy moons (Section IV.A). The modularized, high-DOF mechanical configuration (Section IV.B) and the flexible architecture of the NEO Autonomy (Section IV.C) enabled a multitude of different mobility gaits (Section IV.E), which were proven in numerous lab and field tests in a wide range of environmental conditions (Section IV.F), including sand-covered surface, undulating ice, high-slope snow, and vertical glacial hole. It is particularly notable that all these achievements were made by only two robots with the common mechanical configuration driven by the same code base. However, there is still a long way ahead of us to realize the new robotic exploration paradigm we proposed in this paper. The hardware and software technologies of EELS are still at an early stage of development, and there are many essential capabilities that still need to be implemented, such as automated adaptation and behavioral evolution. Our progress was a small step, but it could one day make a ‘giant leap’ for revolutionizing robotic space exploration and enable us to go where no robots have gone before.

### Acknowledgments

The research was carried out at the Jet Propulsion Laboratory, California Institute of Technology, under a contract with the National Aeronautics and Space Administration (80NM0018D0004). Reference herein to any specific commercial product, process, or service by trade name, trademark, manufacturer, or otherwise, does not constitute or imply its endorsement by the United States Government or the Jet Propulsion Laboratory, California Institute of Technology.

### References

- Artemis III Science Definition Team. 2020. "Artemis III Science Definition Team Report: A Bold New Era of Human Discovery."
- Bland, M. T., T. L. Becker, K. L. Edmundson, Th Roatsch, B. A. Archinal, B. A. Takir, and et al. 2018. "'A New Enceladus Global Control Network, Image Mosaic, and Updated Pointing Kernels from Cassini's 13-Year Mission." *Earth and Space Science*.
- Bouton, Arthur, William Reid, Travis Brown, Adriana Daca, Mielad Sabzehi, and Hari Nayar. 2023. "Experimental Study of Alternative Rover Configurations and Mobility Modes for Planetary Exploration." *IEEE Aerospace Conference*.
- Brown, H. M., A. K. Boyd, B. W. Denevi, M. R. Henriksen, M. R. Manheim, M. S. Robinson, E. J. Speyerer, and R. V. Wagner. 2022. "Resource potential of lunar permanently shadowed regions." *Icarus*.
- Chodas, Mark, Masahiro Ono, Jessica Weber, Laura Rodriguez, Michael Ingham, Ben Hockman, Karl Mitchell, Morgan Cable, and Jason Rabinovitch. 2023. "Enceladus Vent Explorer Mission Architecture Trade Study." *IEEE Aerospace Conference*.
- Chu, Lauren E., Kyle M. Brown, and Kristo Kriechbaum. 2017. "Mars 2020 Sampling and Caching Subsystem Environmental Development Testing and Preliminary Results." *IEEE Aerospace Conference*.
- Daddi, Guglielmo, Tiago S. Vaquero, Ashkan Jasour, Michael Paton, Marlin Strub, Mitch Ingham, Masahiro Ono, and Rohan Thakker. n.d. "Risk-aware Integrated Task and Motion Planning for Resilient Mobility under Localization Failures with Chance Constraints." *Under review for IEEE Robotics and Automation Letters*.

- Drevinskas, Tomas, A. C. Noell, M. S., Mora, M. F. Ferreira Santos, Willis, P. A., M. L. Cable, T. A. Nordheim, and M Ono. 2023. "Design and Integration of an Underwater Oceans Analyzer Into the EELS Robot System." *Lunar and Planetary Science Conference (LPSC)*.
- Drevinskas, Tomas, Aaron Noell, Florian Kehl, Konstantin Zamuruyev, Mauro Ferreira Santos, Maria Mora, Travis Boone, et al. 2023. "A gravity-independent single-phase electrode reservoir for capillary electrophoresis applications." *Electrophoresis*.
- Drevinskas, Tomas, Maria Mora, Mauro Ferreira Santos, Aaron Noell, and Peter Willis. 2023. "Submersible Capillary Electrophoresis Analyzer: A Proof-of-Concept Demonstration of an In Situ Instrument for Future Missions to Ocean Worlds ." *Analytical Chemistry*.
- Farley, Ken. 2015. *Mars 2020 Project Update for Committee on Astrobiology and Planetary Science*. [https://sites.nationalacademies.org/cs/groups/ssbsite/documents/webpage/ssb\\_169425.pdf](https://sites.nationalacademies.org/cs/groups/ssbsite/documents/webpage/ssb_169425.pdf).
- Georgiev, Nikola. 2023. "Efficiency Estimation and Optimization of Multistage Compound Planetary Gearboxes and Application to the Design of the Active Skin Propulsion of EELS." *International Conference on Intelligent Robots and Systems*.
- Georgiev, Nikola, Torkom Pailevanian, Eric Ambrose, Avak Archanian, Hovhannes Melikyan, Daniel Loret de Mola Lemu, and Matthew Gildner. 2024. "EELS: A Modular Snake-like Robot Featuring Active Skin Propulsion, Designed for Extreme Icy Terrains." *Proceedings of the IEEE Aerospace Conference*.
- Gildner, Matthew, Nikola Georgiev, Eric Ambrose, Torkom Pailevanian, Avak Archanian, Hovhannes Melikyan, Loret Loret de Mola Lemu, and Masahiro Ono . 2024. "To Boldly Go Where No Robots Have Gone Before – Part 2: The Versatile Mobility of the EELS Robot for Robustly Exploring Unknown Environments." *Submitted to AIAA SciTech*.
- Hand, Kevin. 2020. *Alien oceans: the search for life in the depths of space*.
- Hand, Kevin, D. Berisford, T. Daimaru, T. Foster, and J. Hofmann. 2020. "Penitente formation is unlikely on Europa." *Nature Geoscience* 13 (1).
- Hobley, D. E., J. M. Moore, A. D. Howard, and O. M. Umurhan. 2018. "Formation of metre-scale bladed roughness on Europa's surface by ablation of ice." *Nature Geoscience* 11 (12): 901-904.
- Hockman, Benjamin, Smith Miles, Samuel Howell, Adarsh Rajguru, Emily Klonicki, Yoseph Bar-Cohen, Terry Hendricks, David Woerner, and Jean-Pierre Fleurial. 2022. "PRIME: "Probe using Radioisotopes for Icy Moons Exploration" - A Comprehensive Cryobot Architecture for Accessing Europa's Ocean." *Astrobiology Science Conference (AbSciCon)*.
- Jain, Abhinandan. 2019. "DARTS - Multibody Modeling, Simulation and Analysis Software." In *Multibody Dynamics*, by Francisco Geu Flores (ed.) Andrés Kecskeméthy. Springer.
- Jayne, Bruce C. 2020. "What Defines Different Modes of Snake Locomotion?" *Integrative & Comparative Biology*.
- Jia, Xianzhe, Margaret G. Kivelson, Krishan K. Khurana, and William S. Kurth. 2018. "Evidence of a plume on Europa from Galileo magnetic and plasma wave signatures." *Nature Astronomy*.
- Kite, Edwin S., and Allan M. Rubin. 2016. "Sustained eruptions on Enceladus explained by turbulent dissipation in tiger stripes." *Geophysical Research Letters*.
- Laurence, David. 2017. "A tale of two poles: Toward understanding the presence, distribution, and origin of volatiles at the polar regions of the Moon and Mercury." *Journal of Geophysical Research: Planets*.
- Luyken, Jörg. 2023. "Watch: Oktoberfest waitress carries 13 beer steins at once." *The Telegraph*. 9 25. <https://www.telegraph.co.uk/world-news/2023/09/25/watch-oktoberfest-waitress-carries-13-steins-to-customers/>.
- MacKenzie, Shannon, Marc Neveu, Alfonso Davila, Jonathan Lunine, Kathleen Craft, Morgan Cable, Charity Phillips-Lander, et al. 2021. "The Enceladus Orbilander Mission Concept: Balancing Return and Resources in the Search for Life." *PSJ\_IOPscience-header.png*.
- Marteau, Eloïse, Luis Phillippe Tosi, Marcel Veismann, Peter Gavrilov, Benjamin Hockmann, Masahiro Ono, Maisha Khanum, Mohammad Abdelrahim, and Hamid Marvi. 2024. "To Boldly Go Where No Robots Have Gone Before – Part 3: The Screw Mobility System of EELS for Robust Surface and Subsurface Mobility on Highly Unknown Terrains." *AIAA SciTech 2024*.
- Mier-Hicks, Fernando, Håvard Fjær Grip, Arash Kalantari, Scott Moreland, Benjamin Pipenberg, Matthew Keennon, Timothy K. Canham, et al. 2023. "Sample Recovery Helicopter." *IEEE Aerospace Conference*.
- Mitchell, Karl, Jason Rabinovitch, Jonathan Scamardella, and Morgan Cable. 2023. "A Proposed Cryovolcanic Eruption Model for Enceladus' Plume." *Under Review. Authorea Preprint* . <https://doi.org/10.22541/essoar.168988431.17819793/v1>.
- Mitchell, Karl, Masahiro Ono, Carolyn Parcheta, and Saverio Iacoponi. 2017. "Dynamic pressure at Enceladus' vents and implications for vent and conduit in-situ studies." 48th Lunar and Planetary Science Conference.

- Moeller, Robert C., Louise Jandura, Keith Rosette, Matt Robinson, Jessica Samuels, Milo Silverman, Kyle Brown, and et. al. 2021. "The Sampling and Caching Subsystem (SCS) for the Scientific Exploration of Jezero Crater by the Mars 2020 Perseverance Rover." *Space Science Review*.
- Moravec, Hans. 1988. *Mind Children*. Harvard University Press.
- Nakajima, Miki, and Andrew P. Ingersoll. 2016. "Controlled boiling on Enceladus. 1. Model of the vapor-driven jets." *Icarus*.
- NASA/JPL-Caltech. 2023. *Meet the Mars Samples: Roubion (Sample 1)*. June 21. <https://mars.nasa.gov/resources/27520/meet-the-mars-samples-roubion-sample-1/>.
- National Academies of Sciences, Engineering, and Medicine. 2022. "Origins, Worlds, and Life: A Decadal Strategy for Planetary Science and Astrobiology 2023-2032."
- Ono, Masahiro, Brandon Rothrock, Eduardo Almeida, Adnan Ansar, Richard Otero, Andres Huertas, and Matthew Heverly. 2016. "Data-driven surface traversability analysis for Mars 2020 landing site selection." *IEEE Aerospace Conference*.
- Ono, Masahiro, Mitchel Karl, Aaron Parness, Kalind Carpenter, Iacoponi Saverio, Ellie Simonson, Aaron Curtis, et al. 2018. "Enceladus vent explorer concept." In *Outer Solar System: Prospective Energy and Material Resources*, 665-717. Springer.
- Otsu, Kyohei, Guillaume Matheron, Sourish Ghosh, Olivier Toupet, and Masahiro Ono. 2019. "Fast approximate clearance evaluation for rovers with articulated suspension systems." *Journal of Field Robotics*.
- Paton, Michael, Richard Rieber, Sarah Yearicks, Matthew Gildner, Masahiro Ono, and et al. 2024. "2023 EELS Field Tests at Athabasca Glacier as an Icy Moon Analog Environment." *IEEE Aerospace Conference*.
- Peters, Gregory H., William Abbey, Gregory Bearman, Gregory Mungas, J. Anthony Smith, Robert C. Anderson, Susanne Douglas, and Luther W. Beegle. 2008. "Mojave Mars simulant—Characterization of a new geologic Mars analog." *Icarus*.
- Porco, Carolyn, Daiana DiNino, and Francis Nimmo. 2014. "How the geysers, tidal stresses, and thermal emission across the south polar terrain of enceladus are related." *Astronomical Journal* 148 (3).
- Prior-Jones, Michael, Elizabeth Bagshaw, and et al. 2017. "Cryoegg: Development and field trials of a wireless subglacial probe for deep, fast-moving ice." *Journal of Glaciology*.
- Rankin, Arturo, Mark Maimone, Jeffrey Biesiadecki, Nikunj Patel, Dan Levine, and Olivier Toupet. 2020. "Driving Curiosity: Mars Rover Mobility Trends During the First Seven Years." *IEEE Aerospace Conference*.
- Reid, William, Gareth Merion-Griffith, Sisir Karumanchi, Blair Emanuel, Brendan Chamberlain-Simon, Joseph Bowkett, and Michael Garrett. 2021. "Actively Articulated Wheel-on-Limb Mobility for Traversing Europa Analogue Terrain." *Field and Service Robotics: Results of the 12th International Conference*.
- Reid, William, Michael Paton, Sisir Karumanchi, Brendan Chamberlain-Simon, Blair Emanuel, and Gareth Merion-Griffith. 2020. "Autonomous Navigation over Europa Analogue Terrain for an Actively Articulated Wheel-on-Limb Rover." *International Conference on Intelligent Robots and Systems*.
- Reid, William, Tara Bartlett, Arthur Bouton, Marlin P. Strub, Michael Newby, Stephan Gerdts, Joshua Martin, Scott Moreland, and Ryan McCormick. 2024. "Planning and Control for Autonomous Drives of the Mars Sample Recovery Helicopter." *To appear in the Proceedings of IEEE Aerospace Conference*.
- Roden-Reynolds, Devin C, Megan H Walker, Camille R Wasserman, and Jesse C Dean. 2015. "Hip proprioceptive feedback influences the control of mediolateral stability during human walking." *Journal of neurophysiology*.
- Schenk, P. M., R. N. Clark, C. J. A. Howett, A. J. Verbiscer, and J. H. (Eds) Waite. 2018. *Enceladus and the Icy Moons of Saturn*. Tucson, AZ.: University of Arizona Press.
- Sparks, W. B., K. P. Hand, M. A. McGrath, E. Bergeron, M. Cracraft, and S. E. Deustua. 2016. "Probing for Evidence of Plumes on Europa with HST/STIS." *The Astrophysical Journal*.
- Talbot, William, Jeremy Nash, Michael Paton, Eric Ambrose, Brandon Metz, Rohan Thakker, Rachel Etheredge, Masahiro Ono, and Viorela Ila. 2023. "Principled ICP Covariance Modelling in Perceptually Degraded Environments for the EELS Mission Concept." *International Conference on Intelligent Robots and Systems (IROS)*.
- Thakker, Rohan, Michael Paton, Marlin Strub, Michael Swan, and et al. 2024. "To Boldly Go Where No Robots Have Gone Before – Part 4: NEO Autonomy for Robustly Exploring Unknown, Extreme Environments with high-DOF Robots." *AIAA SchTech*.
- Thakker, Rohan, Michael Paton, Marlin Strub, Michael Swan, Guglielmo Daddi, and et al. 2023. "EELS: Towards Autonomous Mobility in Extreme Terrain with a Versatile Snake Robot with Resilience to Exteroception Failures." *International Conference on Intelligent Robots and Systems (IROS)*.
- Thomas, P.C., J.A. Burns, P. Helfenstein, S. Squyres, J. Veverka, C. Porco, E.P. Turtle, et al. 2007. "Shapes of the Saturnian icy satellites and their significance." *Icarus*.

- Toupet, Olivier, Tyler Del Sesto, Masahiro Ono, Steven Myint, Joshua Vander Hook, and Michael McHenry. 2020. "A ROS-based Simulator for Testing the Enhanced Autonomous Navigation of the Mars 2020 Rover." *IEEE Aerospace Conference*.
- Tuthill, John C, and Eiman Azim. 2018. "Proprioception." *Current Biology*.
- Vance, S.D., K.L. Craft, E. Shock, and et al. 2023. "Investigating Europa's Habitability with the Europa Clipper." *Space Science Reviews*.
- Vaquero, Tiago S., Guglielmo Daddi, Rohan Thakker, Michael Paton, Ashkan Jasour, and et al. n.d. "Autonomous Task and Motion Planning for Ice Worlds Exploration." *Under review, Science Robotics*.
- Verma, Vandi, Mark Maimone, Dan Gaines, R. Francis, Tara Estlin, Stephan Kuhn, G. R. Rabideau, et al. 2023. "Autonomous Robotics is Driving Perseverance Rover's Unprecedented Progress on Mars." *Science Robotics* 8 (80).
- Villanueva, G.L., H.B. Hammel, S.N. Milam, and et al. 2023. "JWST molecular mapping and characterization of Enceladus' water plume feeding its torus." *Nature Astronomy*.
- Zimmerman, W., R. Bonitz, and J. Feldman. 2001. "Cryobot: an ice penetrating robotic vehicle for Mars and Europa." *IEEE Aerospace Conference*.